Journal of Biomolecular NMR, 3 (1993) 127–132
ESCOM

J-Bio NMR 109

3D ^{13}C–^{15}N-heteronuclear two-spin coherence spectroscopy for polypeptide backbone assignments in ^{13}C–^{15}N-double-labeled proteins

Thomas Szyperski, Gerhard Wider, John H. Bushweller and Kurt Wüthrich*

Institut für Molekularbiologie und Biophysik, Eidgenössische Technische Hochschule-Hönggerberg, CH-8093 Zürich, Switzerland

Received 16 December 1992
Accepted 18 December 1992

Keywords: NMR; Resonance assignments; Heteronuclear two-spin coherence spectroscopy; Protein structure determination

SUMMARY

The pulse sequence of a new constant-time 3D triple-resonance experiment, ct-HA[CAN]HN, is presented. This experiment delineates exclusively scalar connectivities and uses $^{13}C^{\alpha}$–^{15}N heteronuclear two-spin coherence to overlay the chemical shift evolution periods of the $^{13}C^{\alpha}$ and ^{15}N nuclei, thereby providing the four resonance frequencies of the α-proton, the α-carbon, the amide nitrogen, and the amide proton of a given amino acid residue in three dimensions. This experiment promises to be a valid alternative to 4D experiments, providing the same information on intraresidue polypeptide backbone connectivities in ^{13}C–^{15}N-double-labeled proteins.

Sequence-specific ^{1}H NMR assignments, which provide the basis for 3D protein structure determinations in solution (Wüthrich et al., 1982), have conventionally been obtained by analysis of ^{1}H–^{1}H sequential NOEs (Wüthrich, 1986). Although work with homonuclear ^{1}H NMR is usually limited to proteins with molecular weights below 10 000 to 12 000, this strategy can be applied to larger proteins with the use of isotope labeling and higher-dimensional, heteronuclear-resolved [^{1}H,^{1}H]-NOESY experiments (e.g., Torchia et al., 1989; Wüthrich et al., 1991). As an alternative, sequential assignments have been obtained using exclusively heteronuclear scalar couplings along the polypeptide backbone in ^{13}C–^{15}N-double-labeled proteins (Bax et al., 1990;

* To whom correspondence should be addressed.

Abbreviations: 3D, 4D, three-dimensional, four-dimensional; TPPI, time-proportional phase incrementation; ct, constant-time; rf, radiofrequency; NOE, nuclear Overhauser enhancement; NOESY, two-dimensional nuclear Overhauser enhancement spectroscopy; glutaredoxin(C14S), mutant *E. coli* glutaredoxin with the cysteine at position 14 replaced by serine.

Ikura et al., 1990; Bax and Ikura, 1991; Clubb et al., 1992), whereby the heteronuclear 4D NMR experiments HACANHN (Boucher and Laue, 1992) and HNNCAHA (Kay et al., 1992) have been developed for obtaining the intraresidue polypeptide backbone connectivities. However, as has been noted by Kay et al. (1992), because of the short $^{13}C^{\alpha}$ T_2 relaxation times in larger molecules, these 4D NMR experiments are applicable only for proteins with molecular weights below approximately 15 000, where the limited spectral overlap hardly requires a fourth dimension. As an alternative, we propose a 3D experiment with evolution of heteronuclear ^{13}C–^{15}N two-spin coherence and simultaneous evolution of the ^{15}N and ^{13}C chemical shifts, which provides the magnetization transfer pathway outlined in Fig. 1. In the resulting 3D spectrum the $^1H^{\alpha}$, $^{13}C^{\alpha}$, ^{15}N and $^1H^N$ chemical shifts of a given residue are encoded in two peaks rather than in the single peak detected in the aforementioned 4D spectra (Boucher and Laue, 1992; Kay et al., 1992), but otherwise the same information is obtained. Advantages of the reduced dimensionality include that the smaller data set facilitates data handling and processing, that larger values of t_{max} can be chosen for the indirect dimensions, and that more extensive phase cycling is feasible within the same total accumulation time, resulting in improved suppression of artefacts.

The scheme for the 3D ct-HA[CAN]HN experiment is shown in Fig. 2. In the following description of the magnetization transfer by product-operator formalism (Sørensen et al., 1983), the spin operators are I^{α} for $^1H^{\alpha}$, N for the amide ^{15}N nucleus, A for the $^{13}C^{\alpha}$ nucleus, and I^N for $^1H^N$. Relaxation terms and constant multiplication factors will be omitted, and we retain only those product-operator terms that result in observable magnetization during the detection period and only those trigonometric functions that describe the chemical shift evolution. For simplicity, magnetization transfer via the sequential two-bond scalar coupling $^2J(^{13}C_i^{\alpha}, ^{15}N_{i+1})$ is neglected. At time (b) (Fig. 2) the longitudinal α-proton magnetization (1)

$$\sigma(a) = I_z^{\alpha}, \tag{1}$$

is converted into heteronuclear two-spin coherence (2),

$$\sigma(b) = I_x^{\alpha} A_y, \tag{2}$$

provided that τ_1 is set to $1/2\ ^1J(^1H^{\alpha}, ^{13}C^{\alpha})$. In order to minimize losses due to transverse relaxation, the evolution of the $^1H^{\alpha}$ chemical shift is incorporated into the delay, τ_2, used for the generation of antiphase magnetization between ^{15}N and $^{13}C^{\alpha}$, representing a constant-time experiment (Grzesiek and Bax, 1992). τ_2 is set equal to $1/^1J(^{13}C^{\alpha}, ^{13}C^{\beta})$, thereby effectively decoupling $^{13}C^{\alpha}$ from

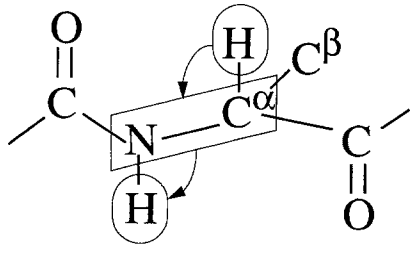

Fig. 1. Magnetization transfer pathway for the ct-HA[CAN]HN experiment. The box indicates that the chemical shifts of the ^{15}N and $^{13}C^{\alpha}$ nuclei evolved simultaneously as heteronuclear two-spin coherence.

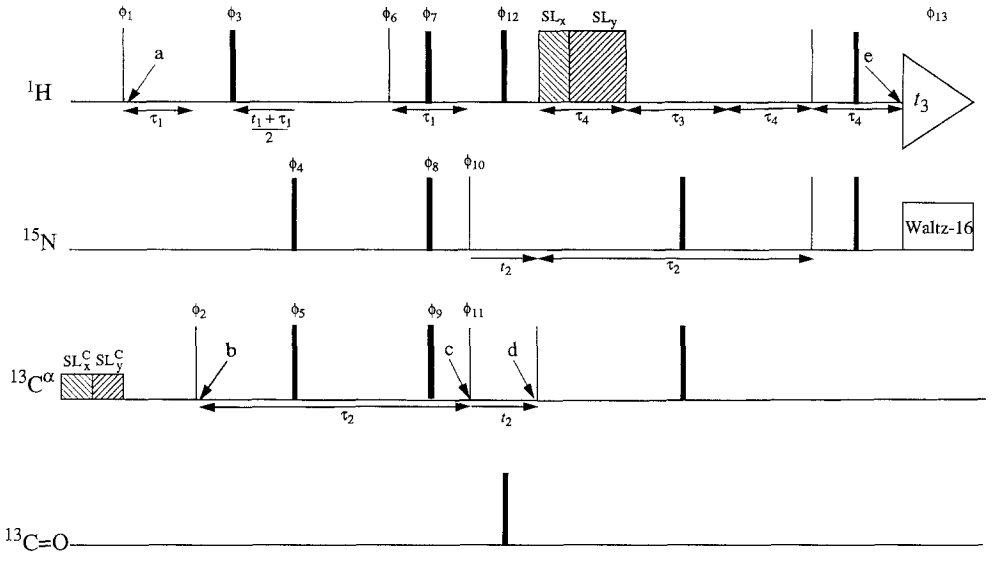

Fig. 2. Experimental scheme of the 3D ct-HA[CAN]HN experiment. For all four rf-channels, 90°- and 180°-pulses are indicated by thin and thick vertical bars, respectively, and the phases are indicated above the pulses. Where no rf-phase is marked, the pulse is applied along +x. The delay τ_1 is tuned to $1/2[^1J(^1H^\alpha,^{13}C^\alpha)]$, τ_2 to $1/[^1J(^{13}C^\alpha,^{13}C^\beta)]$ and τ_4 to $1/2[^1J(^1H^N,^{15}N)]$, with $\tau_3=\tau_2-2\,\tau_4$. Double arrows indicate fixed delays, and single arrows are delays that are incremented during the experiment. A Waltz-16 composite pulse decoupling sequence (Shaka et al., 1983) is used during the proton detection. Two spin-lock pulses, SL_x and SL_y, with an overall duration equal to τ_4, i.e., SL_x=1.8 ms and SL_y=3.8 ms, are used to destroy the proton magnetization, including the water line (Otting and Wüthrich, 1988). The $^{13}C^\alpha$ nuclei are saturated prior to the application of the first proton pulse, using two low-power pulses of 2 ms duration each, SL_x^c and SL_y^c. The phase cycling is: $\phi_1=\phi_{10}$=8(x), ϕ_2=4(x,−x), $\phi_3=\phi_4=\phi_5$=2(x,x,−x,−x), ϕ_6=8(y), $\phi_7=\phi_8=\phi_9=\phi_{12}$=4(x), 4(−x), ϕ_{11}=4(y,−y), ϕ_{13} (receiver)=4(x,−x). Quadrature detection in t_1 and t_2 is accomplished with States-TPPI (Marion et al., 1989) by independently incrementing the groups of phases ϕ_1 and ϕ_3, and ϕ_4, ϕ_8 and ϕ_{10}, respectively. The letters a to e identify stages in the experiment that are referred to in the text. The scheme was developed using the program POMA (Güntert et al., 1992b).

$^{13}C^\beta$. Assuming that $^1J(^{13}C^\alpha,^{13}C^\beta)$ = 35 Jz and $^1J(^{13}C^\alpha,^{15}N) \approx 11$ Hz, τ_2 is thus significantly shorter than $1/2^1J(^{13}C^\alpha,^{15}N)$, but is close to the optimal value if the short $^{13}C^\alpha$ T_2 relaxation times are also considered. During the second τ_1 delay, transverse magnetization of $^{13}C^\alpha$ is refocused with respect to $^1H^\alpha$, so that

$$\sigma(c) = A_y N_z \cos[\Omega(^1H^\alpha)t_1] \quad (3)$$

A 90°-pulse on ^{15}N (ϕ_{10} in Fig. 2) subsequently excites two-spin coherence A_yN_y, while a 90°-purge-pulse (ϕ_{11} in Fig. 2) converts transverse $^{13}C^\alpha$ magnetization, which remains in-phase with respect to the ^{15}N spins because of the imperfect tuning of τ_2 to $^1J(^{13}C^\alpha,^{15}N)$ into longitudinal magnetization. During t_2 the two-spin coherence evolves with both chemical shifts, $\Omega(^{15}N)$ and $\Omega(^{13}C^\alpha)$, while $^1H^\alpha$ and ^{13}C=O are decoupled by 180°-pulses, yielding

$$\sigma(d) = A_yN_y \cos[\Omega(^1H^\alpha)t_1] \cos[\Omega(^{13}C^\alpha)t_2] \cos[\Omega(^{15}N^\alpha)t_2]. \quad (4)$$

A 90°-pulse on $^{13}C^\alpha$ then creates single-quantum coherence on ^{15}N, which is antiphase with

respect to $^{13}C^{\alpha}$. This antiphase magnetization is refocused during the delay, τ_2. Since the overall duration of the two spin-lock purge pulses used to suppress the water signal and to destroy residual proton magnetization (Otting and Wüthrich, 1988) is set to $1/2^1J(^1H^N,^{15}N)$, the ^{15}N magnetization is antiphase with respect to $^1H^N$ at the end of τ_2, and the reverse INEPT leads to

$$\sigma(e) = I_y^N \cos[\Omega\,(^1H^{\alpha})t_1] \cos[\Omega\,(^{13}C^{\alpha})t_2] \cos[\Omega\,(^{15}N)t_2]. \quad (5)$$

Using the addition theorems for trigonometric functions, $\sigma(e)$ can be re-written as

$$\sigma(e) = I_y^N \cos[\Omega\,(^1H^{\alpha})t_1] \{\cos\{[\Omega\,(^{15}N) + \Omega\,(^{13}C^{\alpha})]t_2\} + \cos\{[\Omega\,(^{15}N) - \Omega\,(^{13}C^{\alpha})]t_2\}\} \quad (6)$$

Phase-sensitive detection of both the double-quantum and zero-quantum components contained in the two-spin coherence requires the generation of the corresponding imaginary term (7)

$$\sigma^i(e) = I_y^N \cos[\Omega\,(^1H^{\alpha})t_1] \{\sin\{[\Omega\,(^{15}N) + \Omega\,(^{13}C^{\alpha})]t_2\} + \sin\{[\Omega\,(^{15}N) - \Omega\,(^{13}C^{\alpha})]t_2\}\}. \quad (7)$$

This is achieved by applying the States-TPPI method (Marion et al., 1989) to all pulses on ^{15}N applied before t_2 (ϕ_4, ϕ_8 and ϕ_{10} in Fig. 2). This phase-incrementation yields

$$\sigma(e) = I_y^N \cos[\Omega\,(^1H^{\alpha})t_1] \cos[\Omega\,(^{13}C^{\alpha})t_2 \sin[\Omega\,(^{15}N)t_2], \quad (8)$$

which is, according to the addition theorems for trigonometric functions, equal to Eq. 7. Thus the complex aquisition of the two-spin coherence leads to the observation of $\Omega(^{15}N) \pm\Omega\,(^{13}C^{\alpha})$ along ω_2.

As a practical application, we recorded a 3D ct-HA[CAN]HN spectrum of a 4 mM solution of a mixed disulfide formed between ^{13}C–^{15}N-double-labeled mutant *E. coli* glutaredoxin(C14S) and glutathione (Bushweller et al., 1992). Figure 3 shows a 2D cross section at a fixed $^1H^{\alpha}$ chemical shift. Each pair of peaks along the ν_2 axis in this cross section encodes the four backbone resonance frequencies of $^1H^{\alpha}$,$^1H^N$,$^{13}C^{\alpha}$ and ^{15}N for a particular residue: the $^1H^{\alpha}$ and $^1H^N$ chemical shifts are obtained directly from the peak positions in the 3D spectrum, the center of each peak pair yields the offset of the amide nitrogen from the ^{15}N carrier frequency, and the separation of the two peaks is equal to twice the offset of the α-carbon from the ^{13}C carrier frequency. In principle, it is therefore possible to obtain the intraresidue backbone assignments of $^1H^{\alpha}$,$^{13}C^{\alpha}$,^{15}N and ^1H from this 3D spectrum for all residues except Gly and Pro. In the presently studied protein, glutaredoxin(C14S), all $^1H^{\alpha}$ and $^{13}C^{\alpha}$ resonances could be assigned with the sole exceptions of the six Gly, the three Pro and Gln[66], which is not observable due to exchange broadening (J.H. Bushweller, M. Billeter, A. Holmgren and K. Wüthrich, unpublished results). Relatively weak signals were obtained for β-sheet residues with large values of $^3J_{\alpha\beta}$, i.e., residues with large values of both $^3J_{HN\alpha}$ and $^3J_{\alpha\beta}$. Additional connectivities arising from the sequential two-bond scalar coupling, $^2J(^{13}C_i^{\alpha}, ^{15}N_{i+1})$, were observed for a few residues located in flexible parts of the protein (Sodano et al., 1991). Overall, this experiment with a protein of molecular weight 11 000 confirms the statement in the introductory paragraph that 3D HA[CAN]HN provides the same information as the 4D HACANHN (Boucher and Laue, 1992) or 4D HNNCAHA (Kay et al., 1992) experiments. Applications of practical interest may be wherever poor ^1H chemical shift

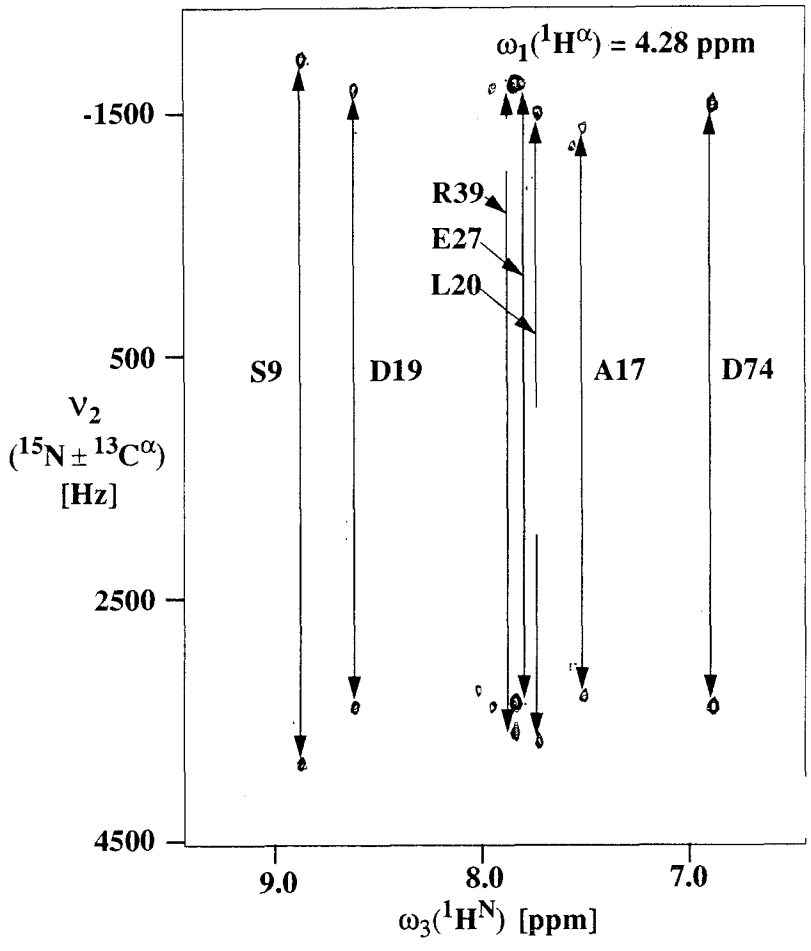

Fig. 3. Contour plot of a crossplane in a 3D ct-HA[CAN]HN spectrum taken at the $^1H^\alpha$ chemical shift value of 4.28 ppm along ω_1. The spectrum was recorded with a 4 mM solution of a mixed disulfide formed between the recombinant mutant *E. coli* glutaredoxin(C14S) and glutathione (Bushweller et al., 1992) in 90% H_2O/10%D_2O, pH=6.5, at T=20 °C. The glutaredoxin(C14S) was uniformly labeled with ^{13}C and ^{15}N. A Bruker AMX 600 spectrometer equipped with a fourth rf-channel was used. $25(t_1)*154(t_2)*1024(t_3)$ complex points were accumulated, with t_{1max}=10.0 ms, t_{2max}=12.5 ms and t_{3max}=131 ms. Eight scans per time increment were acquired, resulting in a total measuring time of 45 h. The carrier frequencies of the ^{15}N and $^{13}C^\alpha$ pulses were set to 105.1 ppm and 40.1 ppm, respectively. Phase-sensitive detection was achieved using States-TPPI (Marion et al., 1989) in t_1 and t_2. The data were processed using the program PROSA (Güntert et al., 1992a). The time domain data in the t_1 and t_2 dimensions were extended by linear prediction to 32 and 256 complex points, respectively. Prior to Fourier transformation the data were multiplied with a cosine window (DeMarco and Wüthrich, 1976). The axis along ν_2 was scaled such that the sum of the carrier frequencies of ^{15}N and ^{13}C (211.7 MHz at 14.1 T) defined 0 Hz.

dispersion requires isotope labeling with ^{15}N and ^{13}C even for relatively small proteins, e.g., for structure determinations with purely α-helical proteins, or for investigation of partially unfolded proteins which may exhibit proton chemical shifts that are close to the 'random coil' values (Neri et al., 1992).

ACKNOWLEDGEMENTS

Financial support was obtained from the Schweizerischer Nationalfonds (project 31.32033.91) and the U.S. National Institutes of Health (postdoctoral fellowship to J.H.B.). We thank R. Marani for the careful processing of the manuscript.

REFERENCES

Bax, A., Ikura, M., Kay, L.E., Torchia, D.A. and Tschudin, R. (1990) *J. Magn. Reson.*, **86**, 304–318.
Bax, A. and Ikura, M. (1991) *J. Biomol. NMR*, **1**, 99–104.
Boucher, W. and Laue, E.D. (1992) *J. Am. Chem. Soc.*, **114**, 2262–2264.
Bushweller, J.H., Åslund, F., Wüthrich, K. and Holmgren, A. (1992) *Biochemistry*, **31**, 9288–9293.
Clubb, R.T., Thanabal, V. and Wagner, G. (1992) *J. Biomol. NMR*, **2**, 203–210.
DeMarco, A. and Wüthrich, K. (1976) *J. Magn. Reson.*, **24**, 201–204.
Grzesiek, S. and Bax, A. (1992) *J. Magn. Reson.*, **96**, 432–440.
Güntert, P., Dötsch, V., Wider, G. and Wüthrich, K. (1992a) *J. Biomol. NMR*, **2**, 619–629.
Güntert, P., Schäfer, N., Otting, G. and Wüthrich, K. (1992b) *J. Magn. Res.*, in press.
Ikura, M., Bax, A. and Kay, L.E. (1990) *Biochemistry*, **29**, 4659–4667.
Kay, L.E., Wittekind, M., McCoy, M.A., Friedrichs, M.S. and Mueller, L. (1992) *J. Magn. Reson.*, **98**, 443–450.
Marion, D., Ikura, M., Tschudin, R. and Bax, A. (1989) *J. Magn. Reson.*, **85**, 393–399.
Neri, D., Billeter, M., Wider, G. and Wüthrich, K. (1992) *Science*, **257**, 1559–1563.
Otting, G. and Wüthrich, K. (1988) *J. Magn. Reson.*, **76**, 569–574.
Sodano, P., Bushweller, J.H., Björnberg, O., Holmgren, A., Billeter, M. and Wüthrich, K. (1991) *J. Mol. Biol.*, **221**, 1311–1324.
Shaka, A.J., Keeler, J., Frenkiel, T. and Freeman, R. (1983) *J. Magn. Reson.*, **52**, 335–338.
Sørensen, O.W., Eich, G.W., Levitt, M.H., Bodenhausen, G. and Ernst, R.R. (1983) *Prog. Nucl. Magn. Reson. Spectrosc.*, **16**, 163–192.
Torchia, D.A., Sparks, S.W. and Bax, A. (1989) *Biochemistry*, **28**, 5509–5524.
Wüthrich, K. (1986) *NMR of Proteins and Nucleic Acids*, Wiley, New York.
Wüthrich, K., Wider, G., Wagner, G. and Braun, W. (1982) *J. Mol. Biol.*, **155**, 311–319.
Wüthrich, K., Spitzfaden, C., Memmert, K., Widmer, H. and Wider, G. (1991) *FEBS Lett.*, **285**, 237–247.